

Coherent Communication with Linear Optics

Mark M. Wilde and Todd A. Brun

*Communication Sciences Institute, Department of Electrical Engineering,
University of Southern California, Los Angeles, California 90089*

Jonathan P. Dowling and Hwang Lee

*Hearne Institute for Theoretical Physics, Department of Physics and Astronomy,
Louisiana State University, Baton Rouge, Louisiana 70803*

(Dated:; Received text; Revised text; Accepted text; Published text)

We show how to implement several continuous-variable coherent protocols with linear optics. Noise can accumulate when implementing each coherent protocol with realistic optical devices. Our analysis bounds the level of noise accumulation. We highlight the connection between a coherent channel and a nonlocal quantum nondemolition interaction and give two new protocols that implement a coherent channel. One protocol is superior to a previous method for a nonlocal quantum nondemolition interaction because it requires fewer communication resources. We then show how continuous-variable coherent superdense coding implements two nonlocal quantum nondemolition interactions with a quantum channel and bipartite entanglement. We finally show how to implement continuous-variable coherent teleportation experimentally and provide a way to verify the correctness of its operation.

Keywords: coherent communication, quantum information theory, continuous variables, quantum optics

I. INTRODUCTION

Quantum information theory employs a plethora of resources that aid in communication [1]. Classical communication and entanglement partner together in quantum teleportation to create a noiseless quantum channel between a sender and receiver [2]. Quantum communication and entanglement partner in superdense coding to create two noiseless classical channels between sender and receiver [3]. It is possible to combine the resources of classical communication, quantum communication, and entanglement in a variety of ways to send classical or quantum information [4, 5].

Harrow introduced a new element to quantum information theory: the coherent bit channel [6]. The coherent bit channel is the following isometry

$$|x\rangle^A \rightarrow |x\rangle^A |x\rangle^B : x \in \{0, 1\}. \quad (1)$$

An arbitrary qubit $|\psi\rangle^A = \alpha|0\rangle^A + \beta|1\rangle^A$ becomes the following state

$$\alpha|0\rangle^A|0\rangle^B + \beta|1\rangle^A|1\rangle^B \quad (2)$$

after sending it through the cobit channel. The operation of the cobit channel is similar to the “quantum encoder” [7].

The coherent bit channel or “cobit” channel is fundamentally different from classical communication, quantum communication, or entanglement, but has connections to all three of the above resources. Harrow originally interpreted the cobit channel as a coherent version of a classical channel. He defined it as a quantum feedback operation in which the sender essentially becomes the environment in a dephasing channel. The cobit channel is similar to quantum communication because

a quantum state encodes the transmitted message. The cobit channel thus maintains coherent superpositions of quantum states. This interpretation is the root of the cobit channel’s name [8]. The cobit channel has links to entanglement because protocols that employ it typically consume less entanglement than their incoherent counterparts [6]. Some protocols such as coherent teleportation even generate entanglement in a certain sense [6].

The cobit channel proves useful in constructing coherent implementations of established quantum communication protocols. It gives coherent versions of remote state preparation, teleportation, dense coding, distributed unitaries [6], and entanglement-assisted quantum codes [9, 10]. The cobit channel is also useful as an intermediate step in several quantum information-theoretic proofs [11, 12] and gives the capacity of a unitary gate [13]. Both the direct construction of coherent protocols and the employment of the cobit channel in quantum information-theoretic proofs affirm its status as a fundamental primitive for quantum communication.

A theory of a continuous-variable coherent channel recently emerged [14]. This theory incorporates the effect of finitely squeezed states in continuous-variable quantum information processing [15, 16]. The continuous-variable coherent channel produces coherent versions of continuous-variable teleportation [17] and continuous-variable superdense coding [18, 19]. The continuous-variable coherent channel should prove useful as a resource for continuous-variable communication protocols or in proving various capacities for a continuous-variable quantum channel.

Theoretical quantum information needs experiment to validate its predictions. The field of quantum information will be successful only through incremental demonstrations of quantum communication protocols. Furu-

sawa, et al., pushed the field of quantum information ahead by performing a continuous-variable teleportation experiment [20] that validated the predictions in Ref. [17]. The advantage of the experiment is that its implementation requires linear optics—passive optical elements, offline squeezers, homodyne detection, feedforward classical signaling, and conditional displacements. Several experimentalists have since implemented continuous-variable superdense coding using linear optics [21, 22]. The major advantage that continuous-variable quantum information possesses right now is the ease with which experimentalists can create and control the modes of the electromagnetic field. Continuous-variable quantum information therefore provides an ideal testbed for validating theoretical predictions.

In this work, we give an explicit proposal for a linear-optical experiment to implement the coherent protocols previously outlined [14]. Our proposals make extensive use of the scheme by Filip, Marek, and Andersen (FMA) for a quantum nondemolition interaction [23]. We give a noise model that bounds the performance of the protocols when using FMA’s scheme. The schemes and analysis in this work should provide a clear path for implementing the coherent channel.

We also provide an additional interpretation of a coherent channel as a nonlocal quantum nondemolition interaction. This interpretation suggests that the coherent channel is useful for distributed quantum computation.

We give two new protocols that implement a continuous-variable coherent channel. One of these protocols (CCAEC) requires fewer communication resources than a protocol previously outlined by Filip [24].

We structure our work as follows. Our review in Section II includes the definition of the discrete-variable and continuous-variable coherent channels. Our review in Section III gives FMA’s scheme for a quantum nondemolition interaction [23] because our linear-optical schemes employ this technique. In Section IV, we outline three different ways to implement a continuous-variable coherent channel with linear optics. Coherent superdense coding is the last of these implementations, it is the most efficient in its use of resources, and it is equivalent to implementing two nonlocal quantum nondemolition interactions. Section V shows how to implement continuous-variable coherent teleportation with linear optics. We finally provide a loss analysis for each coherent protocol. These losses are due to finite squeezing, inefficient photodetectors, and inefficient feedforward control.

II. DEFINITIONS

We first review the discrete-variable coherent channel. Harrow defines a classical bit channel from a sender Alice to a receiver Bob as the following isometry:

$$|x\rangle^A \rightarrow |x\rangle^E |x\rangle^B : x \in \{0, 1\}. \quad (3)$$

The channel is classical because the environment correlates with Alice’s state. Thus the channel does not maintain coherent superpositions. The coherent channel supposes that Alice regains the environment’s state—earning its alias as the quantum feedback operation. It is the following isometry:

$$|x\rangle^A \rightarrow |x\rangle^A |x\rangle^B : x \in \{0, 1\}. \quad (4)$$

The cobit channel is similar to classical copying because it copies the basis states while maintaining coherent superpositions.

The above definition tempts one to define a continuous-variable coherent channel as the following map:

$$|x\rangle^A \rightarrow |x\rangle^A |x\rangle^B : x \in \mathbb{R}. \quad (5)$$

The above states are position-quadrature or momentum-quadrature eigenstates. The problem with the above definition is that it requires an infinite amount of energy to implement. It requires infinite energy to copy the eigenstates because they have continuous degrees of freedom. The above coherent channel is therefore an idealized limit. Consider the effect of sending an arbitrary state $|\psi\rangle = \int \psi(x) |x\rangle dx$ through the ideal coherent channel. The resulting state $\int \psi(x) |x\rangle^A |x\rangle^B dx$ is not normalizable and thus has infinite energy. We therefore set aside the ideal coherent channel, and instead use a definition that allows for finitely-squeezed states.

We turn to the Heisenberg picture to formulate the definition in terms of the quadrature operators of the electromagnetic field. The definition has a parameter ϵ that determines the performance of the coherent channel and indicates how much squeezing is present in the channel.

Definition 1 *An ϵ -approximate position-quadrature coherent channel $\tilde{\Delta}_X$ is any mechanism by which one mode transforms to two modes:*

$$[\hat{x}_A \ \hat{p}_A] \xrightarrow{\tilde{\Delta}_X} [\hat{x}_{A'} \ \hat{p}_{A'} \ \hat{x}_{B'} \ \hat{p}_{B'}]. \quad (6)$$

It maintains the canonical commutation relations:

$$[\hat{x}_{A'}, \hat{p}_{A'}] = [\hat{x}_{B'}, \hat{p}_{B'}] = i. \quad (7)$$

It maps the input quadrature operators to the output quadrature operators as follows:

$$\hat{x}_{A'} = \hat{x}_A, \quad (8)$$

$$\hat{x}_{B'} = \hat{x}_A + \hat{x}_{\Delta_X}, \quad (9)$$

$$\hat{p}_{A'} = \hat{p}_A + \hat{p}_{\Delta_X}, \quad (10)$$

where

$$\langle \hat{x}_{\Delta_X} \rangle = \langle \hat{p}_{\Delta_X} + \hat{p}_{B'} \rangle = 0. \quad (11)$$

The condition in (9) indicates that the position quadrature \hat{x}_A copies to mode B' with the addition of some noise \hat{x}_{Δ_X} . The condition in (10) indicates back action in the

momentum quadrature $\hat{p}_{A'}$. The parameter ϵ bounds the performance of the channel by bounding the noise terms as follows:

$$\langle \hat{x}_{\Delta_X}^2 \rangle \leq \epsilon, \quad \langle (\hat{p}_{\Delta_X} + \hat{p}_{B'})^2 \rangle \leq \epsilon. \quad (12)$$

A coherent channel is similar to a nonlocal quantum nondemolition interaction. Suppose that Alice has a mode A , Bob has a mode B , and that Alice and Bob are spacelike separated. A position-quadrature nonlocal quantum nondemolition interaction implements the following transformation

$$\begin{aligned} \hat{x}_A &\rightarrow \hat{x}_A, & \hat{p}_A &\rightarrow \hat{p}_A - g\hat{p}_B, \\ \hat{x}_B &\rightarrow \hat{x}_B + g\hat{x}_A, & \hat{p}_B &\rightarrow \hat{p}_B, \end{aligned} \quad (13)$$

where g is the gain of the interaction. A coherent channel has more restrictions than a nonlocal quantum nondemolition interaction. The coherent channel begins with only one mode. It requires the final gain of the interaction to be unity. It further requires both output position quadratures to be ϵ -close in mean-squared distance. A quantum nondemolition interaction merely requires the second quadrature to have information about the first quadrature. However, it is still useful to consider this connection. Observe the output quadratures in Definition 1. The original position quadrature \hat{x}_A copies to the output quadrature $\hat{x}_{B'}$. The output momentum-quadrature $\hat{p}_{A'}$ also has back-action noise encapsulated in the operator \hat{p}_{Δ_X} . One party possesses the first mode and the other party possesses the second mode. This behavior is similar to the behavior in a nonlocal quantum nondemolition interaction.

The definition for a momentum-quadrature coherent channel is similar to Definition 1. It is useful to have a momentum-quadrature coherent channel definition to observe the similarities between coherent protocols [14] and their incoherent counterparts [17, 18, 19].

Definition 2 *An ϵ -approximate momentum-quadrature coherent channel $\tilde{\Delta}_P$ performs the following transformation with conditions:*

$$\begin{aligned} [\hat{x}_A \ \hat{p}_A] \xrightarrow{\tilde{\Delta}_P} [\hat{x}_{A''} \ \hat{p}_{A''} \ \hat{x}_{B''} \ \hat{p}_{B''}], & \quad (14) \\ [\hat{x}_{A''}, \hat{p}_{A''}] = [\hat{x}_{B''}, \hat{p}_{B''}] = i, & \\ \hat{p}_{A''} = \hat{p}_A, & \\ \hat{p}_{B''} = \hat{p}_A + \hat{p}_{\Delta_P}, & \\ \hat{x}_{A''} = \hat{x}_A + \hat{x}_{\Delta_P}, & \\ \langle \hat{p}_{\Delta_P} \rangle = \langle \hat{x}_{\Delta_P} + \hat{x}_{B''} \rangle = 0, & \\ \langle \hat{p}_{\Delta_P}^2 \rangle, \langle (\hat{x}_{\Delta_P} + \hat{x}_{B''})^2 \rangle \leq \epsilon. & \end{aligned}$$

A coherent channel is useful for implementing a coherent teleportation protocol. The parameter ϵ indicates the performance of the coherent channel in a coherent teleportation protocol [14]. Continuous-variable teleportation schemes have several different performance bounds [17, 25, 26]. The performance bounds are relevant lower

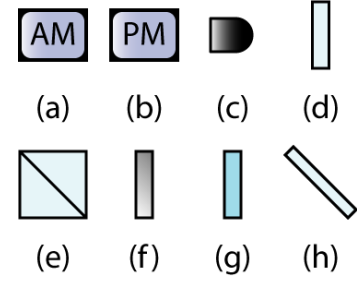


FIG. 1: (Color online) We outline the elements used in our optical circuits. (a) An amplitude modulator displaces the position quadrature of an optical mode. A classical control signal controls the amount of displacement. (b) A phase modulator kicks the momentum quadrature of an optical mode. A classical signal also controls it. (c) A photodetector. (d) A phase shifter. (e) A polarizing beam splitter. (f) A mirror. (g) A half-wave plate with variable transmittivity. (h) A beam splitter.

bounds for the average fidelity of teleporting an arbitrary coherent state. The preparation-and-measurement limit is $1/2$ [17] and the no-cloning limit is $2/3$ [25, 26]. The coherent-state-averaged fidelity for coherent teleportation exceeds $1/2$ if $\epsilon < 1$. The original paper on continuous-variable coherent communication only considered this bound of $1/2$ [14]. Examination of the equations in [14] indicates that the coherent-state-averaged fidelity exceeds $2/3$ if $\epsilon < 1/2$.

III. FMA'S QUANTUM NONDEMOLITION INTERACTION

The coherent protocols originally outlined in Ref. [14] require a quantum nondemolition interaction for their implementation. Quantum nondemolition interactions typically involve an online nonlinear interaction such as a Kerr medium [27]. These online nonlinear interactions are difficult to control experimentally.

FMA provided an experimental proposal for implementing both a squeezer and a quantum nondemolition interaction with linear optics [23]. Experimentalists have implemented both the squeezing transformation [28] and the quantum nondemolition interaction [29] with reasonable performance.

Figure 1 highlights the elements used in a linear-optical circuit. Figure 2 gives the optical circuit for implementing FMA's measurement-induced quantum nondemolition interaction. FMA's scheme uses two offline squeezed modes, three homodyne measurements, and feedforward control.

FMA's scheme is similar in spirit to the Knill, Laflamme, and Milburn scheme for discrete variables [30] though FMA's scheme has the advantage that it is deterministic rather than probabilistic.

The scheme for a quantum nondemolition interaction

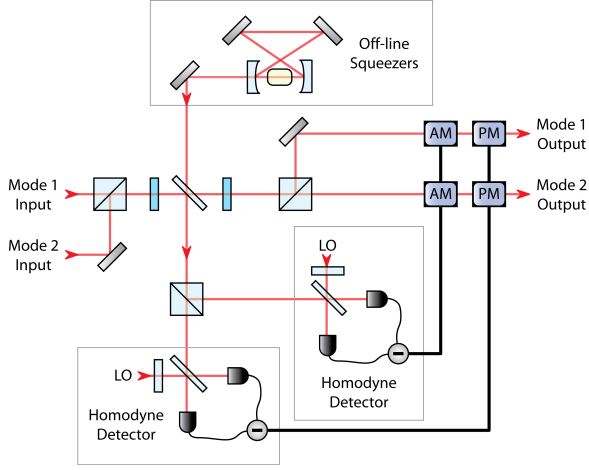


FIG. 2: (Color online) FMA's linear-optical scheme for a quantum nondemolition interaction [23]. LO is an abbreviation for “local oscillator.” The two input modes are orthogonally polarized. The circuit uses two offline squeezers, homodyne detection, and feedforward control to give a quantum nondemolition interaction with unity transfer gain.

is valuable for any continuous-variable quantum computation or communication device. A recent work used it in an algorithm for constructing linear-optical encoding circuits for continuous-variable quantum error correction [31]. We use it in all of our coherent protocols below.

We review the operation of FMA's scheme. The circuit uses two offline squeezers to implement a quantum nondemolition interaction with unity transfer gain. It begins with a polarizing beam splitter combining the two inputs into one spatial mode. A half-wave plate with transmittivity T_1 mixes the two polarization modes. A beamsplitter then combines the spatial mode and the outputs of two offline squeezers. The outputs of the offline squeezers are two orthogonally polarized modes squeezed in conjugate quadratures \hat{x}_B and \hat{p}_A . We measure the outputs of the beamsplitter with two homodyne detectors. The two phase shifters for the local oscillators control which quadrature we measure and thus which quadrature is the nondemolition variable. We send the rightward output of the beamsplitter through a half-wave plate with transmittivity T_2 . FMA require setting the parameters T_1 and T_2 as follows

$$T_1 = 1/(1+T), \quad T_2 = T/(1+T). \quad (15)$$

to have unity transfer gain. A polarizing beamsplitter separates the output of the half-wave plate into two spatial modes. We finally perform modulation of both modes using the results of the homodyne detection.

The above operations transform the input quadrature observables $\hat{x}_1, \hat{p}_1, \hat{x}_2, \hat{p}_2$ to the final output quadrature

observables $\hat{x}'_1, \hat{p}'_1, \hat{x}'_2, \hat{p}'_2$ as follows:

$$\begin{aligned} \hat{x}'_1 &= \hat{x}_1 - \sqrt{\alpha}\hat{x}_0 - \sqrt{\beta}\hat{x}_B, \\ \hat{p}'_1 &= \hat{p}_1 - \left(\frac{1}{\sqrt{T}} - \sqrt{T}\right)\hat{p}_2 + \sqrt{\alpha/T}\hat{p}_0 + \sqrt{T}\beta\hat{p}_A, \\ \hat{x}'_2 &= \hat{x}_2 + \left(\frac{1}{\sqrt{T}} - \sqrt{T}\right)\hat{x}_1 - \sqrt{\alpha/T}\hat{x}_0 + \sqrt{T}\beta\hat{x}_B, \\ \hat{p}'_2 &= \hat{p}_2 - \sqrt{\alpha}\hat{p}_0 + \sqrt{\beta}\hat{p}_A. \end{aligned} \quad (16)$$

Parameter T controls the strength of the interaction. The parameters α and β determine the efficiency of the interaction. The quadratures \hat{x}_0 and \hat{p}_0 are independent and commuting vacuum contributions. We set $T = (3 - \sqrt{5})/2$ for our purposes throughout this work. This setting ensures unity gain for every quantum nondemolition interaction so that

$$\frac{1}{\sqrt{T}} - \sqrt{T} = 1. \quad (17)$$

The above method adds noise to each mode in both quadrature observables. The parameters α and β are as follows

$$\beta = \frac{1-T}{1+T} = \frac{-1+\sqrt{5}}{5-\sqrt{5}}, \quad (18)$$

$$\alpha = \frac{(1-T)(1-\eta)}{(1+T)\eta} = \beta \left(\frac{1-\eta}{\eta} \right). \quad (19)$$

where η is the efficiency of the photodetectors. Let η_F denote the total efficiency of FMA's scheme. We define η_F to be a bound on the second moment of the added noise for the quantum nondemolition interaction

$$\eta_F = \beta((1-\eta)/\eta T + e^{-2r}), \quad (20)$$

where r is the strength of the offline squeezers. We use this bound throughout our work to quantify the performance of FMA's quantum nondemolition interaction.

IV. PRACTICAL IMPLEMENTATIONS OF A COHERENT CHANNEL

Definition 1 for a continuous-variable coherent channel is rather abstract. It gives a set of conditions that a coherent channel must satisfy and is also broad in its scope. The conditions are necessary to implement a coherent superdense coding protocol and are sufficient to implement a coherent teleportation protocol [14]. We illuminate the abstract definition of a coherent channel in this section by providing several ways to implement it. We also further highlight the connection between a coherent channel and a nonlocal quantum nondemolition interaction.

A. Quantum Nondemolition Interaction

The simplest method of implementing a coherent channel is with a quantum nondemolition interaction. Suppose that a sender Alice possesses a mode A that she

wants to send through a coherent channel. She creates a position-squeezed ancilla mode B with squeezing strength r . The Heisenberg-picture observables corresponding to the two-mode state are as follows

$$\hat{x}_A, \hat{p}_A, \hat{x}_B^{(0)} e^{-r}, \hat{p}_B^{(0)} e^r, \quad (21)$$

where the observables \hat{x}_A and \hat{p}_A are her original modes and the observables $\hat{x}_B^{(0)}$ and $\hat{p}_B^{(0)}$ have the fluctuations of the vacuum. It is implicit throughout this work that any quadrature with (0) in the superscript has the fluctuations of the vacuum. Alice performs a quantum non-demolition interaction on her two modes so that the observables evolve as follows:

$$\hat{x}_A, \hat{p}_A - \hat{p}_B^{(0)} e^r, \hat{x}_B^{(0)} e^{-r} + \hat{x}_A, \hat{p}_B^{(0)} e^r. \quad (22)$$

She sends the second mode over a quantum channel to a receiver Bob.

The above operations satisfy the requirements for an (e^{-2r}) -approximate position-quadrature coherent channel. They satisfy constraint (8) because the position quadrature of Alice's final mode is equal to the position quadrature of Alice's original mode. They satisfy constraint (10) because the momentum quadrature of Alice's final mode is equal to the momentum quadrature of Alice's original mode plus a noise term $-\hat{p}_B^{(0)} e^r$ so that $\hat{p}_{\Delta x} = -\hat{p}_B^{(0)} e^r$. They satisfy constraint (9) because the position quadrature of Bob's final mode is equal to the position quadrature of Alice's original mode plus a noise term $\hat{x}_B^{(0)} e^{-r}$ so that $\hat{x}_{\Delta x} = \hat{x}_B^{(0)} e^{-r}$.

Examination of the transformation in (13) confirms that the above protocol also implements a nonlocal quantum nondemolition interaction. This interpretation is rather obvious given that Alice performs the interaction locally and sends one mode over a quantum channel.

Suppose we implement the needed quantum nondemolition interaction with FMA's method. Then the coherent channel is ϵ -approximate where

$$\epsilon = \beta ((1 - \eta) / \eta T + e^{-2r}) + e^{-2r}. \quad (23)$$

The channel is useful if photodetector efficiency $\eta \rightarrow 1$ and squeezing strength r becomes large so that ϵ becomes small.

This particular method of implementing a coherent channel is somewhat wasteful in its usage of resources because a quantum channel implements the coherent channel. We later discuss two methods that make more efficient usage of resources. The first method is coherent communication assisted by entanglement and classical communication (CCAEC). The second is coherent superdense coding. CCAEC uses one classical channel and one bipartite entangled state to implement a coherent channel. Coherent superdense coding uses one bipartite entangled state and one quantum channel to implement two coherent channels.

B. Coherent Communication Assisted by Entanglement and Classical Communication (CCAEC)

Another method for implementing a coherent channel is CCAEC. It uses bipartite entanglement and classical communication to implement a coherent channel. We first give a brief description of the discrete-variable protocol and follow with the continuous-variable description.

Suppose Alice has a qubit $|\psi\rangle^A = \alpha|0\rangle^A + \beta|1\rangle^A$ that she wants to send through a coherent channel. Suppose further that Alice and Bob possess an ebit where Alice has qubit A_1 and Bob qubit B . Alice appends an ancilla $|0\rangle^{A_2}$ and performs a CNOT between A_1 and A_2 . The resulting state is entangled so that the global state is as follows:

$$|\psi\rangle^A \left(|0\rangle^{A_1} |0\rangle^{A_2} |0\rangle^B + |1\rangle^{A_1} |1\rangle^{A_2} |1\rangle^B \right) / \sqrt{2}. \quad (24)$$

Alice performs a Bell measurement on qubits A and A_1 . She performs teleportation-like corrective operations [2] on her qubit A_2 using the two bits resulting from the Bell measurement. The resulting state is a uniform mixture of the following two pure states:

$$\alpha|0\rangle^{A_2} |0\rangle^B + \beta|1\rangle^{A_2} |1\rangle^B, \quad (25)$$

$$\alpha|0\rangle^{A_2} |1\rangle^B + \beta|1\rangle^{A_2} |0\rangle^B. \quad (26)$$

Alice sends Bob one bit so that he can perform a corrective Pauli X operation. The resulting state is as follows

$$\alpha|0\rangle^{A_2} |0\rangle^B + \beta|1\rangle^{A_2} |1\rangle^B, \quad (27)$$

so that Alice and Bob simulate a coherent channel from qubit A_1 to qubits A_2 and B .

The continuous-variable method for CCAEC is similar to continuous-variable teleportation [17], a continuous-variable teleportation network [32, 33], and continuous-variable quantum telecloning [34] though the protocol differs from all of the above protocols in different ways. It differs from continuous-variable teleportation because we use three-mode entanglement shared among two parties. It differs from the teleportation network because we have only two parties instead of three parties. It also differs from the teleportation network because it implements a coherent channel rather than a quantum channel. The protocol is perhaps most similar to quantum telecloning. But it differs from it because we have two parties instead of three. The entanglement in our protocol is GHZ-like, but quantum telecloning employs W-like entanglement.

Now let us describe the continuous-variable protocol. Suppose that Alice possesses a mode A that she wants to transmit through a coherent channel. Alice and Bob possess a three-mode entangled state. Alice possesses the first two modes A_1 and A_2 and Bob possesses the last mode B . We assume that a three-port device called a "tritter" creates the entanglement necessary for the protocol [32, 33]. The entanglement that results from the

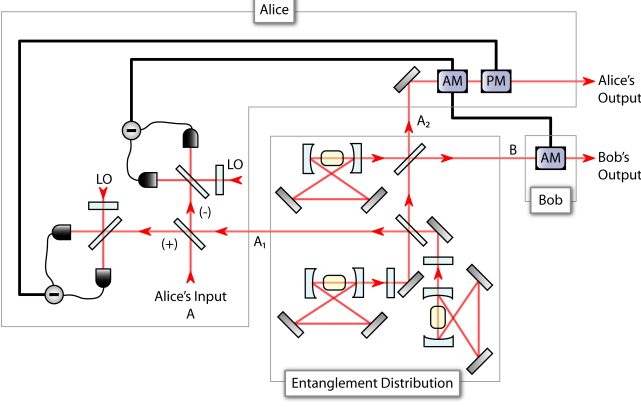


FIG. 3: (Color online) Coherent channel implemented with entanglement and classical communication. The protocol has similarities to previous protocols [17, 32, 33, 34], but has significant differences as well. Alice and Bob share a three-mode entangled state. Alice possesses the first two modes and Bob possesses the third. Alice has a mode A that she wants to send through a coherent channel. She performs teleportation-like measurements on mode A and her first mode in the entangled state. She performs feedforward control on her second mode of the entangled state. She sends one variable over a classical communications channel so that Bob can perform feedforward control. The resulting state is equivalent to one sent through a coherent channel.

tritter is equivalent to the state from [32]. The following correlations hold for modes A_1 , A_2 , and B

$$\begin{aligned}\hat{x}_{A_1} - \hat{x}_{A_2} &= \sqrt{3/2}e^{-r}\hat{x}_2^{(0)} - \sqrt{2^{-1}}e^{-r}\hat{x}_3^{(0)} \\ \hat{x}_{A_2} - \hat{x}_B &= \sqrt{2}e^{-r}\hat{x}_3^{(0)} \\ \hat{p}_{A_1} + \hat{p}_{A_2} + \hat{p}_B &= \sqrt{3}e^{-r}\hat{p}_1^{(0)}\end{aligned}\quad (28)$$

where $\hat{x}_2^{(0)}$ and $\hat{x}_3^{(0)}$ are the position quadratures of the second and third modes sent through the tritter and $\hat{p}_1^{(0)}$ is the momentum quadrature of the first mode sent through the tritter. Parameter r denotes the squeezing strength of the original three vacuum modes sent through the tritter. We assume that the squeezing strength is the same for all three vacuum modes.

Figure 3 outlines the optical circuit needed for our protocol. It begins by Alice mixing her modes A and A_1 at a beamsplitter. The output Heisenberg-picture observables \hat{x}_\pm , \hat{p}_\pm are as follows:

$$\begin{aligned}\hat{x}_\pm &= (\hat{x}_A \pm \hat{x}_{A_1})/\sqrt{2}, \\ \hat{p}_\pm &= (\hat{p}_A \pm \hat{p}_{A_1})/\sqrt{2}.\end{aligned}$$

The observables of modes A_2 and B are then as follows:

$$\begin{aligned}\hat{x}_{A_2} &= \hat{x}_A - (\hat{x}_{A_1} - \hat{x}_{A_2}) - \sqrt{2}\hat{x}_-, \\ \hat{x}_B &= \hat{x}_A - (\hat{x}_{A_1} - \hat{x}_B) - \sqrt{2}\hat{x}_-, \\ \hat{p}_{A_2} &= \hat{p}_A + (\hat{p}_{A_1} + \hat{p}_{A_2} + \hat{p}_B) - \hat{p}_B - \sqrt{2}\hat{p}_+.\end{aligned}$$

Alice performs a position-quadrature homodyne detection on mode $(-)$ and a momentum-quadrature homodyne detection on mode $(+)$. Suppose the photodetectors have efficiency η . The observables \hat{x}_- and \hat{p}_+ collapse to values x_- and p_+ respectively. Alice modulates mode A_2 locally by displacing the position quadrature by $\sqrt{2}x_-$ and the momentum quadrature by $\sqrt{2}p_+$. She sends the value x_- over a classical communications channel. Bob displaces his position quadrature by an amount $\sqrt{2}x_-$. Let us call the resulting modes A' and B' . The Heisenberg-picture observables are then as follows after they perform the above operations:

$$\begin{aligned}\hat{x}_{A'} &= \hat{x}_A - (\hat{x}_{A_1} - \hat{x}_{A_2}) - \sqrt{2(1-\eta)/\eta}\hat{x}_1^{(0)}, \\ \hat{p}_{A'} &= \hat{p}_A + (\hat{p}_{A_1} + \hat{p}_{A_2} + \hat{p}_B) - \hat{p}_B + \sqrt{2(1-\eta)/\eta}\hat{p}_2^{(0)}, \\ \hat{x}_{B'} &= \hat{x}_A - (\hat{x}_{A_1} - \hat{x}_B) - \sqrt{2(1-\eta)/\eta}\hat{x}_1^{(0)}, \\ \hat{p}_{B'} &= \hat{p}_B.\end{aligned}$$

The quadrature operators $\hat{x}_1^{(0)}$ and $\hat{p}_2^{(0)}$ are independent and thus commuting observables. They have the fluctuations of the vacuum and model the inefficiency that both homodyne detectors introduce. Let us determine if the above operations implement a coherent channel. Squeezing introduces some extra noise in mode A_2 . The difference between the position quadratures of modes A_2 and B is as follows:

$$\langle (\hat{x}_{A'} - \hat{x}_{B'})^2 \rangle = 2e^{-2r}.$$

We subtract the original momentum of Alice's mode A from the total momentum of modes A' and B' when considering coherent channel performance according to the performance measure in (12). The quantity $\hat{p}_{A'} + \hat{p}_{B'} - \hat{p}_A$ is as follows:

$$\langle (\hat{p}_{A'} + \hat{p}_{B'} - \hat{p}_A)^2 \rangle = 3e^{-2r} + 2(1-\eta)/\eta.$$

The above operations therefore implement a $(3e^{-2r} + 2(1-\eta)/\eta)$ -approximate position-quadrature coherent channel. The channel becomes ideal as squeezing strength r becomes large and as photodetector efficiency approaches unity.

We can also view the above operations as performing a nonlocal quantum nondemolition interaction. The information in the original position quadrature \hat{x}_A transfers to both modes A' and B' with the addition of some noise. Filip's scheme requires bipartite entanglement and two-way classical communication [24]. Our method requires bipartite entanglement and one-way classical communication. Our scheme is thus an improvement if we view communication as expensive and local operations as free.

C. Coherent Superdense Coding

Braunstein and Kimble proposed a theoretical method for performing continuous-variable superdense coding

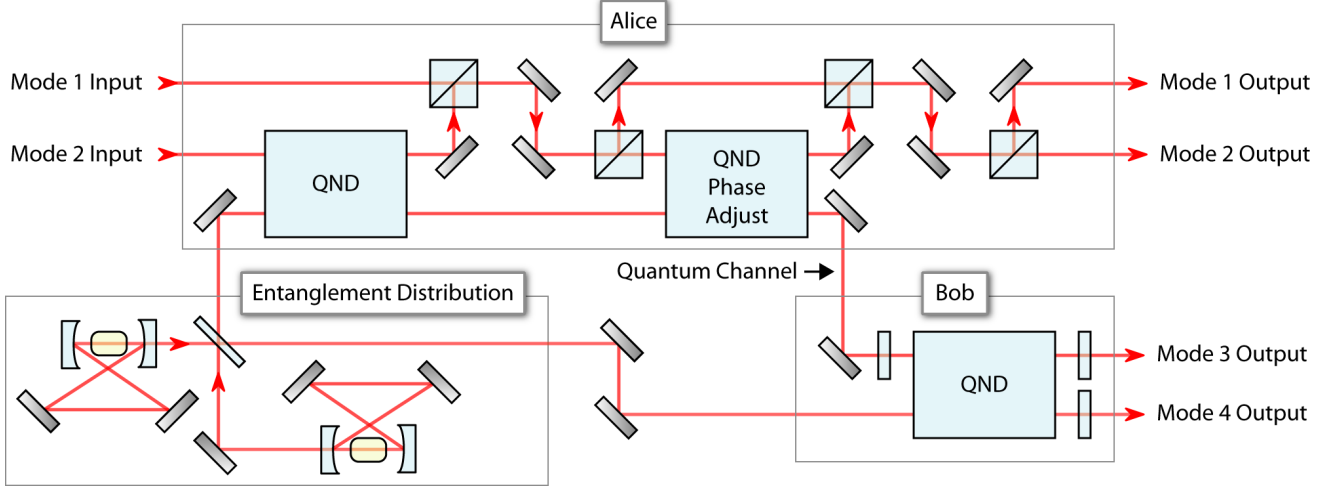


FIG. 4: (Color online) The above linear-optical circuit implements coherent superdense coding or, equivalently, two-nonlocal quantum nondemolition interactions. All phase shifters in the above circuit rotate by π . Alice possesses two modes that she wants to send through a coherent channel. Alice and Bob share two entangled modes. Alice performs some local operations on her two modes and her half of the entangled state. She sends one mode over a quantum channel to Bob. Bob performs some local operations. The resulting states are equivalent to those that would result from Alice sending her two modes through two coherent channels. The states are also equivalent to those that would result from performing two nonlocal quantum nondemolition interactions.

with linear optics [18]. Later work outlined how to make their protocol coherent [14]. We review the theoretical operation of coherent superdense coding briefly and follow with an analysis of losses incurred by employing Filip et al's technique for a quantum nondemolition interaction. Figure 4 gives a way to implement coherent superdense coding experimentally. We also provide two observations concerning coherent superdense coding.

Suppose Alice possesses two modes 1 and 2 at the beginning of the protocol. Alice and Bob also share a two-mode entangled state with Alice having mode three and Bob mode four. The second moment noise of the quadrature observables obey the following inequalities:

$$\langle (\hat{x}_3 - \hat{x}_4)^2 \rangle, \quad \langle (\hat{p}_3 + \hat{p}_4)^2 \rangle \leq \delta.$$

Modes three and four are entangled if $\delta < 1$ [35]. Alice couples her second mode and her half of the entangled state in a quantum nondemolition interaction. She swaps her first mode with her second mode. She couples the second mode with the third mode in a quantum nondemolition interaction. She adjusts the phases of the local oscillators so that the momentum quadrature copies rather than the position quadrature. She sends her third mode over a quantum channel to Bob and swaps her first mode with her second mode. Bob couples the received mode and his half of the entangled state in a quantum nondemolition interaction. This quantum nondemolition interaction subtracts the position quadrature rather than adding it because of the π phase shifters acting on his received mode. He finally sends his last mode through a π phase shifter to reflect its position and momentum quadrature. The resulting four modes have the following

Heisenberg-picture observables:

$$\begin{aligned} \hat{x}'_1 &= \hat{x}_1 - (\hat{x}_2 + \hat{x}_3), \quad \hat{p}'_1 = \hat{p}_1, \\ \hat{x}'_2 &= \hat{x}_2, \quad \hat{p}'_2 = \hat{p}_2 - \hat{p}_3, \\ \hat{x}'_3 &= \hat{x}_2 + \hat{x}_3, \quad \hat{p}'_3 = \hat{p}_1 + (\hat{p}_3 + \hat{p}_4), \\ \hat{x}'_4 &= \hat{x}_2 + (\hat{x}_3 - \hat{x}_4), \quad \hat{p}'_4 = -\hat{p}_4. \end{aligned} \quad (29)$$

Modes one and three satisfy the conditions for an δ -approximate momentum-quadrature coherent channel. Modes two and four satisfy the conditions for an δ -approximate position-quadrature coherent channel. Let us stress that the above operations assume ideal quantum nondemolition interactions.

Consider the effect of using FMA's scheme to implement each quantum nondemolition interaction. Each quantum nondemolition interaction adds noise from two squeezed sources and two vacuum sources due to inefficient homodyne detection. Parameter η_F in (20) bounds the noise that each quantum nondemolition interaction adds. We use three quantum nondemolition interactions in the above protocol. All three quantum nondemolition interactions affect the observables present in the final output modes three and four. Their effects are independent and additive. Therefore using FMA's quantum nondemolition interaction gives two $(\delta + 3\eta_F)$ -approximate coherent channels. These coherent channels are useful if $\delta + 3\eta_F$ is small—less than 1/2 or 1 depending on which teleportation bound we want to surpass.

We make several observations about the above protocol. It reduces to ordinary (incoherent) superdense coding [18] when Alice uses certain input states. Suppose she encodes two classical variables p and x in modes one and

two respectively. She performs this encoding by making modes one and two be highly squeezed in the momentum quadrature and the position quadrature respectively. Modes one and two approach a momentum-quadrature eigenstate $|p\rangle$ and a position-quadrature eigenstate $|x\rangle$ in the infinite squeezing limit. Then Bob's modes three and four are approximately a momentum-quadrature $|p\rangle$ and a position-quadrature eigenstate $|x\rangle$. The noise from finite-squeezing and the quantum nondemolition interactions affect his states so that they are not perfect eigenstates. Bob can perform a measurement to retrieve an approximation of the two classical variables p and x that Alice first sent. Thus this protocol reduces to incoherent dense coding in this sense.

Another way of viewing this protocol is that it implements two nonlocal quantum nondemolition interactions with three local quantum nondemolition interactions. We can view the results as quantum nondemolition interactions because we transfer information about the momentum quadrature \hat{p}_1 to mode three and we transfer information about the position quadrature \hat{x}_2 to mode four. The above coherent superdense coding protocol uses one quantum channel and one set of entangled modes to achieve two nonlocal quantum nondemolition interactions. Coherent superdense coding then is an interesting way to implement two nonlocal quantum nondemolition interactions if we view communication and entanglement as expensive and local operations as free.

V. COHERENT TELEPORTATION

Braunstein and Kimble also gave a theoretical proposal for performing linear-optical continuous-variable teleportation [18]. The later work in [14] illustrated how to make their protocol coherent. We review the operation of coherent teleportation and give a loss analysis when employing FMA's scheme. We also suggest an experimental method with Bell inequalities to determine if coherent teleportation is successful. Figure 5 gives a way to implement coherent teleportation experimentally with linear optics.

Coherent teleportation is a two-party protocol. Alice possesses a mode one that she wants to teleport to Bob. She shares two continuous-variable entangled states with Bob. We label the modes in the first pair as two and three. Alice possesses mode two and Bob possesses mode three. The outputs of the offline squeezers in Figure 5 couple at a beamsplitter to give the first pair of entangled modes. We label the modes in the second pair as four and five. The coherent dense coding circuit requires an entangled pair so modes four and five serve this purpose. Alice possesses mode four and Bob possesses mode five. Both entangled pairs have the following correlations:

$$\begin{aligned} \langle (\hat{x}_2 - \hat{x}_3)^2 \rangle, \quad \langle (\hat{p}_2 + \hat{p}_3)^2 \rangle &\leq \delta, \\ \langle (\hat{x}_4 - \hat{x}_5)^2 \rangle, \quad \langle (\hat{p}_4 + \hat{p}_5)^2 \rangle &\leq \delta. \end{aligned}$$

The above states are entangled if $\delta < 1$.

The protocol begins with Alice sending mode two through a π phase shifter. She couples her modes one and two in a quantum nondemolition interaction. She sends her two modes through the coherent superdense coding circuit in Figure 4. Recall that the first two outputs of the coherent superdense coding circuit belong to Alice and the second two to Bob. Bob combines his mode five from coherent superdense coding and mode three in a quantum nondemolition interaction. He swaps his mode four with the first output of the quantum nondemolition interaction. He then couples his mode four and three in a quantum nondemolition interaction. He adjusts the phases of the local oscillators so that it copies the momentum quadrature rather than the position quadrature. The relations between the input Heisenberg-picture observables and the output observables are as follows:

$$\begin{aligned} \hat{x}'_1 &= \hat{x}_2 - \hat{x}_4, \quad \hat{p}'_1 = \hat{p}_2 + \hat{p}_1, \\ \hat{x}'_2 &= \hat{x}_1 - \hat{x}_2, \quad \hat{p}'_2 = -\hat{p}_2 - \hat{p}_4, \\ \hat{x}'_3 &= \hat{x}_1 + (\hat{x}_3 - \hat{x}_2) + (\hat{x}_4 - \hat{x}_5), \\ \hat{p}'_3 &= \hat{p}_1 + (\hat{p}_2 + \hat{p}_3) + (\hat{p}_4 + \hat{p}_5), \\ \hat{x}'_4 &= \hat{x}_5 - \hat{x}_3, \quad \hat{p}'_4 = \hat{p}_2 + \hat{p}_1 + (\hat{p}_4 + \hat{p}_5), \\ \hat{x}'_5 &= \hat{x}_1 - \hat{x}_2 + (\hat{x}_4 - \hat{x}_5), \quad \hat{p}'_5 = -\hat{p}_5 - \hat{p}_3. \end{aligned}$$

The state in mode one teleports to mode three. The average fidelity F for teleporting a coherent state [20] is as follows

$$F = 2 / \left[\left(\langle (\Delta \hat{x}_{\text{tel}})^2 \rangle + 1 \right) \left(\langle (\Delta \hat{p}_{\text{tel}})^2 \rangle + 1 \right) \right]^{1/2}, \quad (30)$$

where \hat{x}_{tel} and \hat{p}_{tel} are the quadratures of the teleported mode. The fidelity F for coherent teleportation is thus

$$F = 1 / (1 + \delta). \quad (31)$$

Modes one and four are entangled and modes two and five are also entangled because the following correlations hold:

$$\begin{aligned} \langle (\hat{x}'_1 + \hat{x}'_4)^2 \rangle, \quad \langle (\hat{p}'_1 - \hat{p}'_4)^2 \rangle &\leq \delta, \\ \langle (\hat{x}'_2 - \hat{x}'_5)^2 \rangle, \quad \langle (\hat{p}'_2 + \hat{p}'_5)^2 \rangle &\leq \delta. \end{aligned} \quad (32)$$

Consider if we employ FMA's scheme to implement the quantum nondemolition interactions in coherent teleportation. Recall that this scheme adds at most $3\eta_F$ to the second moments of the quadratures in coherent superdense coding. Coherent teleportation requires three extra quantum nondemolition interactions. These interactions each add at most a noise factor of η_F to the second moments of Bob's output quadrature variables. Thus the total noise contribution from six quantum nondemolition interactions is no more than $6\eta_F$. This contribution affects the fidelity of teleportation by bounding it as follows:

$$F > 1 / (1 + \delta + 6\eta_F). \quad (33)$$

- A. Peres, and W. K. Wootters, Phys. Rev. Lett. **70**, 1895 (1993).
- [3] C. H. Bennett and S. J. Wiesner, Phys. Rev. Lett. **69**, 2881 (1992).
- [4] I. Devetak, A. W. Harrow, and A. Winter, Phys. Rev. Lett. **93**, 230504 (2004).
- [5] I. Devetak, A. W. Harrow, and A. Winter, arXiv:quant-ph/0512015 (2005).
- [6] A. Harrow, Phys. Rev. Lett. **92**, 097902 (2004).
- [7] T. B. Pittman, B. C. Jacobs, and J. D. Franson, Phys. Rev. A **64**, 062311 (2001).
- [8] A. W. Harrow and D. W. Leung, Quantum Information and Computation **5**, 380 (2005).
- [9] T. A. Brun, I. Devetak, and M.-H. Hsieh, Science **314**, pp. 436 (2006).
- [10] T. A. Brun, I. Devetak, and M.-H. Hsieh, arXiv:quant-ph/0608027 (2006).
- [11] I. Devetak and J. Yard, arXiv:quant-ph/0612050 (2006).
- [12] J. Yard and I. Devetak, arXiv:0706.2907 (2007).
- [13] A. W. Harrow and P. W. Shor, arXiv:quant-ph/0511219 (2005).
- [14] M. M. Wilde, H. Krovi, and T. A. Brun, Phys. Rev. A **75**, 060303 (2007).
- [15] S. L. Braunstein and A. Pati, eds., *Quantum Information with Continuous Variables* (Springer, 2003).
- [16] S. L. Braunstein and P. van Loock, Rev. Mod. Phys. **77**, 513 (2005).
- [17] S. L. Braunstein and H. J. Kimble, Phys. Rev. Lett. **80**, 869 (1998).
- [18] S. L. Braunstein and H. J. Kimble, Phys. Rev. A **61**, 042302 (2000).
- [19] M. Ban, J. Opt. B: Quantum Semiclass. Opt. **1**, L1 (1999).
- [20] A. Furusawa, J. L. Sorensen, S. L. Braunstein, C. A. Fuchs, H. J. Kimble, and E. S. Polzik, Science **282**, 706 (1998).
- [21] J. Mizuno, K. Wakui, A. Furusawa, and M. Sasaki, Phys. Rev. A **71**, 012304 (pages 4) (2005).
- [22] X. Li, Q. Pan, J. Jing, J. Zhang, C. Xie, and K. Peng, Phys. Rev. Lett. **88**, 047904 (2002).
- [23] R. Filip, P. Marek, and U. L. Andersen, Phys. Rev. A **71**, 042308 (2005).
- [24] R. Filip, Phys. Rev. A **69**, 052313 (2004).
- [25] F. Grosshans and P. Grangier, Phys. Rev. A **64**, 010301(R) (2001).
- [26] C. M. Caves and K. Wodkiewicz, Phys. Rev. Lett. **93**, 040506 (2004).
- [27] P. Grangier, J. A. Levenson, and J.-P. Poizat, Nature **396**, 537 (1998).
- [28] J.-I. Yoshikawa, T. Hayashi, T. Akiyama, N. Takei, A. Huck, U. L. Andersen, and A. Furusawa, arXiv:quant-ph/0702049 (2007).
- [29] J. Yoshikawa, A. Huck, U. L. Andersen, and A. Furusawa, in *Spring meeting of Physical Society of Japan, 19aXG-2* (2007).
- [30] E. Knill, R. Laflamme, and G. Milburn, Nature **409**, 46 (2001).
- [31] M. M. Wilde, H. Krovi, and T. A. Brun, arXiv:0705.4314 (2007).
- [32] P. van Loock and S. L. Braunstein, Phys. Rev. Lett. **84**, 3482 (2000).
- [33] H. Yonezawa, T. Aoki, and A. Furusawa, Nature **431**, 430 (2004).
- [34] P. van Loock and S. L. Braunstein, Phys. Rev. Lett. **87**, 247901 (2001).
- [35] L.-M. Duan, G. Giedke, J. I. Cirac, and P. Zoller, Phys. Rev. Lett. **84**, 2722 (2000).
- [36] K. Banaszek and K. Wódkiewicz, Phys. Rev. A **58**, 4345 (1998).